BIOCHEMICAL FINITE ELEMENT ANALYSIS OF THE LOCKED KIRSCHNER WIRE SYSTEM VERSUS VOLAR PLATE FIXATION OF DISTAL RADIUS FRACTURE

Woraphon Jaroenporn, Wassapol Rerksanan*, Vajarin Phiphobmongkol*, Jaruwat Vechasilp*, Samran Phukang**, Wichit Siritattamrong**, Natcha Ariyaprakai***

***Department of Orthopaedics, Police General Hospital, Bangkok, Thailand**
****Department of Orthopaedics, Jurarat 3 International Hospital, Bangkok, Thailand**

Abstract

Background: Volar locking plate (VP) and Kirschner wire (K-wire) fixations of distal end radius fractures are the most frequently used techniques that produce similar long term clinical results. However, inadequate fixation strength of the K-wire may cause pin loosening or migration. Although these complications can be prevented by immobilization, joint stiffness and a prolonged recovery period can occur.

Objective: Herein, a technique that provided more stability, allowing immediate motion after fixation by linking the K-wires into a single system (locked K-wire system) was proposed.

Methods: We evaluated biomechanical responses of the locked K-wire system and a VP in extra-articular distal radius fracture models AO/OTAa type 23A2 and 23A3 using three-dimensional finite element analysis. All models were tested under axial, bending, and torsional loads.

Results: From the simulation results, the total displacement was greater in the dorsal wedge fracture than that from the simple fracture under all loads for both fixation systems. The locked K-wire system and the VP could withstand immediate physiologic load with maximum displacements of 1.15 mm and 1.39 mm, respectively.

Conclusion: Considering the immediate physiologic load resistance and the ability to preserve its position during the bone-healing period, the locked K-wire system might be used as an alternative to fix distal radius fractures.

Keywords: Finite element analysis, Distal radius fracture, Volar plate, K-wire, Locked K-wire, Biomechanical study

J Southeast Asian Med Res 2021: 5 (2):91-98
https://www.jseamed.org

Correspondence to:
Jaroenporn W, Department of Orthopaedics, Police General Hospital, Bangkok, Thailand
Email address: woraphon.md@gmail.com

Received: 1 August 2021
Revised: 6 September 2021
Accepted: 10 September 2021

Introduction

Distal radius fractures are one of the most common skeletal injuries; their incidence has been increasing worldwide. A shift in favor of surgical treatment has taken place in general. [1–3] The direct economic costs of distal radius fractures in the US are more than USD 480 million annually. [4] Several surgical options are available for distal radius fractures, and the cost of the treatment depends on the choice of fixation. [5] The two most common surgical techniques are Kirschner wire (K-wire) and volar locking plate (VP) fixations. [5,6] VP provides stronger fixation that facilitates early motion and early return to work which is still considered more invasive, time-consuming and delays wound healing[5–9]

K-wire fixation is a well-established procedure with many advantages including minimal invasion, rapid application and lower cost of treatment. However, one disadvantage includes the fixation strength, the most concerning drawback, leading to pin loosening or migration. Commonly surgeons resort to immobilization which may lead to stiffness and prolonged recovery. [7, 10, 11] To overcome this limitation, we linked all K-wires that were fixed to a fracture site in one system (locked K-wire system). No further immobilization was needed so patients could immediately perform early range of motion exercises. Although clinical studies comprise the optimum investigations of differences between surgical options, unfortunately, confounding variables are found that are difficult to identify and isolate. Cadaveric studies are limited by the shortage of specimens. Meanwhile, finite element (FE) analysis is commonly used in biomechanical studies because parameters can be adjusted in a more controllable manner. [12, 13] Thus, we used three-dimensional (3D) FE analysis to investigate the biomechanical responses of the VP and locked K-wire systems with two most common fracture patterns of the distal radius under three physiologic load conditions, i.e., bending, axial, and torsional load.

Methods

This study was conducted under Police General Hospital Ethics Committee No. 111/2562. Informed consent was obtained from the subjects enrolled in the study.

Finite element modeling

Computed tomography (CT) was used to scan the right radius bone of a healthy 60-year-old Thai man in a neutral position. Images were taken in the transverse plane at series of 80 scans at 1 mm intervals. The contours of the cancellous and cortical bone were extracted from the set of CT images and imported into Mimics 10.01 (Materialize, Leuven, Belgium) to create three-dimensional radius geometry. To simplify calculations, all soft tissues were excluded. These data were then imported into PowerSHAPE 2016 (Delcam Plc, Birmingham, UK) to create a computer-aided design (CAD) model suitable for meshing. Afterward, a CAD file was used to mesh an FE model in an FE package (ANSYS, V 15.0, Ansys Inc., Canonsburg, PA, USA) to generate the solid bone model. The summary of model creation is shown in **Figure 1**.

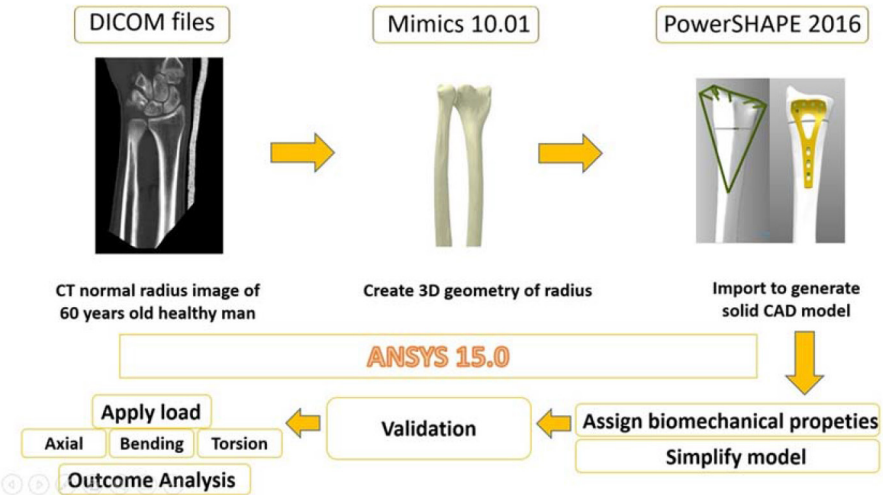

Figure 1. Approach of FE analysis

To simulate the distal radius fracture, the fracture pattern was assumed to be one of two types, namely, metaphyseal or dorsal wedge fractures, according to the 23-A2 classification of the AO surgery reference (**Figure 2**). [14] First, an undisplaced fracture with impaction but no abnormal palmar or dorsal tilt was made with a fracture gap of 1 mm, 25 mm proximal from the distal end of the radius using an idealized planar cut (**Figure 2a**). Then a simple extra-articular with dorsal tilt (Colles fracture) was made with a cut having a 35° wedge toward the dorsal site, 25 mm proximal from the distal end of the radius using an idealized planar cut (**Figure 2b**). Two models were built to compare different fixation techniques, including VP and locked K-wire systems. In the VP model, the plate was created using Titanium Variable Angle LCP Two-Column Volar Distal Radius Plate (2.4, six holes, a width of 22 mm, a length of 54 mm, six head holes, three shaft holes, right, DePuy Synthes, USA) as a template. Thread details of the locking screws were excluded from our model. The screws were bonded with the bone to simulate conditions occurring after osteo-integration. All screws were bonded with the plate to simulate thread clenching with the plate.

For the locked K-wire system, K-wires were created using a stainless-steel K-wire with a diameter of 1.6 mm as a template. Each K-wire was modeled with linear-elastic, 8-noded brick-shaped elements. The locked K-wire system was composed of seven K-wires. The first two K-wires started at the radial styloid tip and passed through the fracture site to the opposite cortex. Three other K-wires were introduced from the dorsal cortex of the lunate fossa and passed through the fracture site to the volar cortex. One K-wire passed parallel just below the articular surface in the coronal plane. The other one was fixed at 10 cm proximal to the articular surface. All protruding parts of the K-wires were assembled in a single unit using the last K-wire as the core (**Figure 3**).

a b

Figure 2. Radius model: (a) simple fracture (23A2); (b) dorsal wedge fracture (23A3)

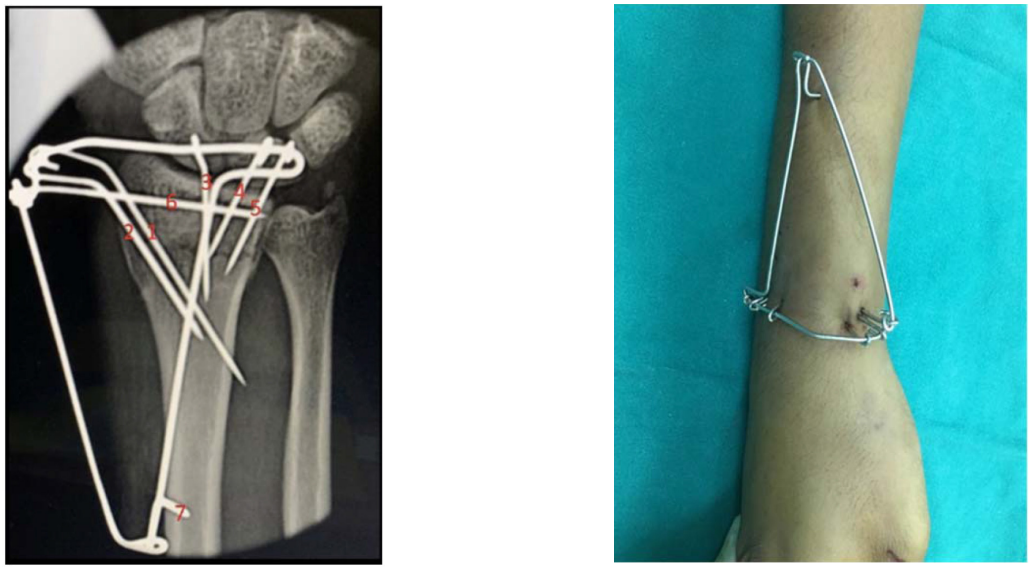

Figure 3. Locked K-wire system consisting of seven pins

Convergence test and model validation

For model verification, a convergence test was used to guarantee that our numerical model reached the converged results and that no further mesh refinement was necessary. The radius FE models were meshed with 1-, 2-, and 3-mm element sizes using quadratic tetrahedral elements (Solid 92) in ANSYS. The cancellous and cortical bones were considered isotropic, linear, and elastic, with elastic moduli of 1.3 GPa and 17 GPa, respectively. Poisson's ratio was set to 0.3. [13, 15] A surface-to-surface gluing contact parameter was inserted at the interface of the cortical bone and cancellous bone, to prevent movement between the meshes of these regions at the interface. The elastic modulus and Poisson's ratio of the titanium plates and screws were 110 GPa and 0.3, respectively. [16]

The proximal end of the model was fixed, and an axial force (compression force) of 100 N was applied at the center of the distal end radius. The maximum displacement, maximum strain, and maximum von Mises stress value at the fracture gap were evaluated for convergence in all models. The tolerance level was set within 5%.

To validate our FE model, the converged results from the model were compared with the experimental results from the fresh cadaveric study and prior FE of distal radius studies. [8, 17]

Finite element analysis

To avoid numerical differences arising due to FE meshing, all models were derived from the same solid model with a single meshed pattern. The resulting FE model was meshed using a 2-mm element size after the convergence test. The element number totaled 58682, 59929, 62588, and 64027 for dorsal wedge fracture with VP, simple fracture with VP, dorsal wedge fracture with locked K-wire, and simple fracture with K-wire, respectively. For VP models, the plate was placed volarly just proximal to the watershed line. A minimal gap between the plate and the bony surface was left to represent the limitation of an actual bone surface. Screws were projected perpendicular to the plate through the bone. Six screws were placed to the head and three were filled in the shaft of the plate (the locking features were removed from the slots). The surface-to-surface gluing contact was inserted at the volar plate-screw and screw-bone. As for the interaction of the K-wire system, the frictional values between K-wire and cortical and cancellous bone were 0.5 and 0.3, respectively. [18, 19] The K-wires were glued to each other.

Biomechanical responses from the VP and the locked K-wire system were investigated under the simulation of the magnitudes and directions of physiologic loads during active wrist joint movement of daily activities. Bending and torsional loads of 1 Nm and an axial load of 100 N, under the boundary condition and the material properties used in the convergence test, were applied at the end of the distal radius. [8, 13, 20] Four FE models, two fracture patterns and two fixation methods, were simulated under three load conditions. To study the load transmission pattern and loosening potential of the fixation, the von Mises stress values, and maximum displacements of the distal radius were recorded.

Results

To avoid geometry distortions, the FE model was meshed using an element size of 2 mm. As for the convergence assessment, the differences in the maximum von Mises stress, displacements, and strain values were less than 5% in our models. For model validation, we compared with the fresh cadaveric distal radius experimental results of the compressive stiffness of 379±146 Nmm^{-1} [17] and from the finite element study of the distal radius of 494 Nmm^{-1} [18], while our result was 478 Nmm^{-1}, indicating that the radius FE model was reliable for further analysis.

The maximum displacements of all models were documented to evaluate the responses of immediate motions after the operation. The dorsal wedge pattern fracture exhibited a larger displacement than the simple fracture regardless of fixation technique. The VP had a larger displacement than the locked K-wire system under the bending force but smaller displacement under axial and torsional forces for both fracture patterns. The maximum displacements of the

locked K-wire system and the VP found in the dorsal wedge pattern were 1.15 mm (torsional force) and 1.39 mm (bending force), respectively (**Figure 4**).

The stress distribution was similarly concentrated around the fracture gap area in all simulated models (**Figure 5**). Regardless of the fracture pattern, the maximum von Mises stress of the VP (σ-VP Max) was the highest under the bending load and the lowest under the compression load. The maximum von Mises stress of the locked K-wire system (σ-LKW Max) was the highest under the torsional load and the lowest under compression load. The locked K-wire system revealed lower stress than the VP only under the bending force (**Figure 6**).

Discussion

In a related study, a similar method of linking K-wires was used, but a metal clamp was used as a linkage in the setting of a hand fracture. Based on the mechanical analysis, that system had significantly greater resistance to flexion and traction loads than a normal K-wire fixation.[21] However, the clamp was not easily available. The simulation results showed that both constructs can withstand immediate postoperative functional loads. The displacement, stiffness and stress values of the VP were similar to those of related studies. The moment force was higher under bending and torsional loads; thus, creating significantly higher displacement and stress values compared with those under axial load.[19,23]

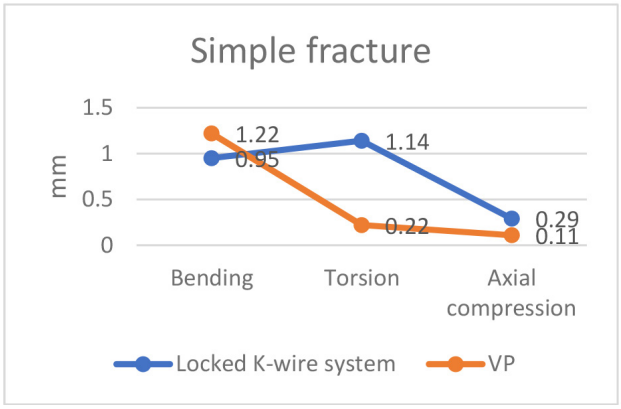

a

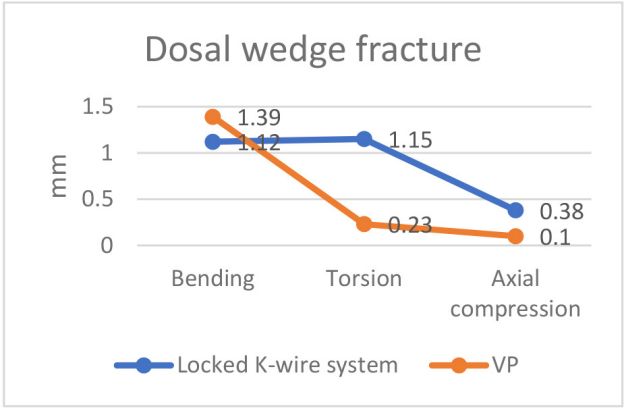

b

Figure 4. Displacement at the fracture site for all simulated models: (a) simple fracture model; (b) dorsal wedge fracture

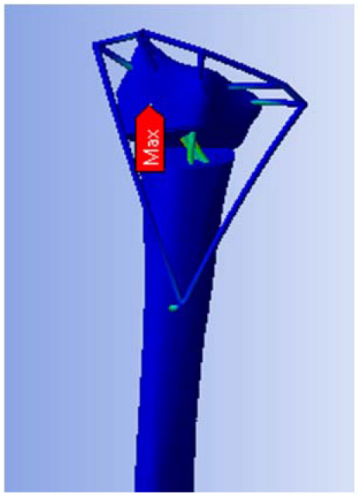

a

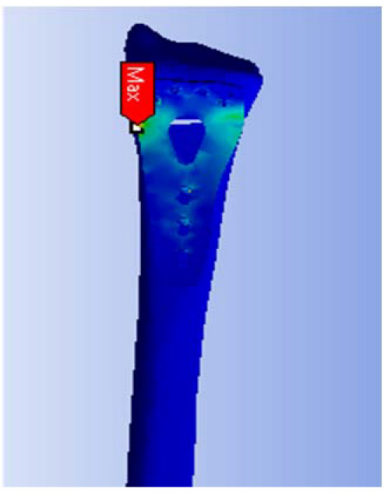

b

Figure 5. Stress distribution and σMax: (a) locked K-wire system; (b) VP system.

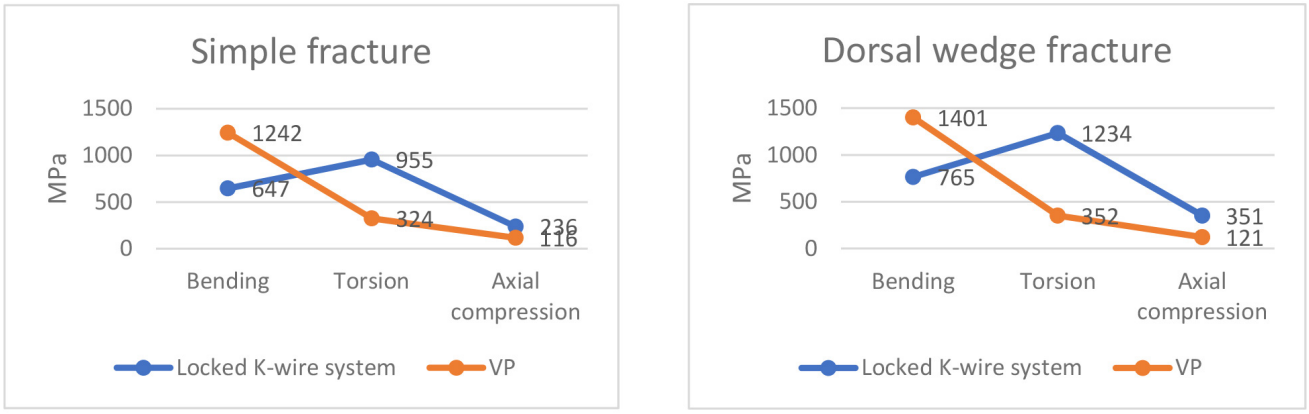

a b

Figure 6. Maximum von Mises stress values for all simulated models: (a) simple fracture model; (b) dorsal wedge fracture.

The VP was a stable fixation for the dorsal wedge fracture that had slightly higher displacement and stress values compared with the simple fracture. [19]

The locked K-wire system had smaller displacement under the bending load conditions. This phenomenon is explained by the structure of the locked K-wires system, which is mainly constructed in the dorsal-volar position, and the increased moment arm, so the resistance to the bending force was enhanced. The largest displacement of the locked K-wire, caused by the torsional force (1.14 mm in the simple fracture and 1.15 mm in the dorsal wedge fracture), was within acceptable limits (**Figure 4**).

When comparing the two systems, the locked K-wire system had smaller displacement and σ-Max than those of the VP system under the bending load conditions. The bending force is considered the most crucial because it tends to separate the fragments, preventing fracture healing. [16, 13, 24] Thus, the locked K-wire system could be considered to exhibit excellent fixation properties.

The highest stress distribution for all the models was localized around the fracture gap, similar to a related study, which could be explained by the load-bearing property of the fixation principle. [19]

Therefore, we used the same principle to design the locked K-wire system without any special instruments. Three reasons for constructing the locked K-wire system included 1) reducing articular surface, 2) supporting radial height, inclination, and dorsovolar tilt, and 3) providing distraction force to resist compressive force. Hence, we used a construct of seven K-wires. The first and second K-wires were used to maintain the radial inclination and height. The next three K-wires were used to perform fine reduction and support the axial load from the articular surface. The sixth K-wire was used to support the articular surface, while the seventh wire was used as a lever to generate a distraction force by locking the extrusion parts of the other K-wires onto itself (**Figure 3**). The linkage technique of K-wires also played an essential role in the strength of the construct. The protruded first six K-wires were made into a small loop in the sagittal plane for the last K-wire to pass through. Thus, better resistance to the dorsovolar bending force of wrist flexion and extension, considered the most important deforming force, was achieved. Then, all the loops were tightened such that the K-wires could not be individually moved, and an ideal single-unit system could be achieved, similar to locking plates.

This study was also designed to compare the biomechanical responses of VP and locked K-wire systems during axial, bending, and torsional loads comprising physiological loadings in daily life activities. [12, 22] The radius model in our study was simulated from a normal bone even though the distal radius fracture was more common in an osteoporotic population. The reason was the variety of the severities of osteoporosis, which consequently changes the elastic modulus and Poisson's ratio. With lower stiffness (from osteoporosis), the biomechanical responses would show a similar tendency; and hence, the results could be applied to osteoporosis cases. [13]

In the clinical setting, once K-wires are linked in the locked K-wire system, we need to tighten every linkage so that it would be nearly impossible to remove a wire individually. The locking facilitates the use of the system and encourages early motion exercises.[7] Even though the locked K-wire system might not be superior to the VP system in every aspect, it remains sufficiently strong to withstand the physiologic force with the additional advantage of the ability to maintain bony alignment until bone union. The locked K-wire system is considered to be a good alternative for distal radius fracture fixation.

Nonetheless, this study encountered limitations of the simplification of numerical convergence considerations. These included the load conditions, which may not represent the realistic tendon force on the wrist joint, implant, and model simplification including bone material properties, screw geometry, and the strength of the linkage between K-wires. These may vary practically depending on the patient and the surgeon's experience which may possibly influence the response accuracy.

Conclusion

Even though the VP system is considered to be the fixation of choice with superior biomechanical properties for distal radius fracture, with appealing biomechanical responses, cost-effectiveness, and the advantage in preventing wire migration, the locked K-wire system proved to be an alternative fixation technique in treating distal radius fractures. One of the main drawbacks of the proposed approach was that some parameters had to be simplified using finite element analysis, which may not truly represent the strength of the fixation. Therefore, in a future study, an actual prototype of the locked K-wire system should be applied to a cadaver to evaluate the biomechanical properties precisely.

Acknowledgment

We sincerely thank the volunteers for providing the radius model from their CT scans.

Conflicts of Interest

The authors declare that they have no conflicts of interest.

References

1. Sander AL, Leiblein M, Sommer K, Marzi I, Schneidmüller D, Frank J. Epidemiology and treatment of distal radius fractures: Current concept based on fracture severity and not on age. Eur J Trauma Emerg Surg 2020; 46: 585–90.
2. Chung KC and Spilson SV. The frequency and epidemiology of hand and forearm fractures in the United States. J Hand Surg Am 2001; 26: 908–15.
3. Koo OT, Tan DM and Chong AK. Distal radius fractures: An epidemiological review. Orthop Surg 2013; 5: 209–13.
4. Chaudhry H, Kleinlugtenbelt YV, Mundi R, Ristevski B, Goslings JC, Bhandari M. Are volar locking plates superior to percutaneous K-wires for distal radius fractures? A meta-analysis. Clin Orthop Relat Res 2015; 473: 3017–27.
5. Costa ML, Achten J, Parsons NR, Rangan A, Griffin D, Tubeuf S, et al. DRAFFT Study Group Percutaneous fixation with Kirschner wires versus volar locking plate fixation in adults with dorsally displaced fracture of distal radius: Randomised controlled trial. BMJ 2014; 349: g4807.
6. Youlden DJ, Sundaraj K, Smithers C. Volar locking plating versus percutaneous Kirschner wires for distal radius fractures in an adult population: A meta-analysis. ANZ J Surg 2019; 89: 821–826.
7. Downing ND, Karantana A. A revolution in the management of fractures of the distal radius? J Bone Joint Surg Br 2008; 90: 1271–75.
8. Zysk A, Lewis G. Finite element analysis study of prototype of a novel intramedullary injectable bioresorbable polymer fixator versus a volar plate for surgical treatment of distal radius fractures. World J Eng Technol 2017; 5: 648–67.
9. Satake H, Hanaka N, Honma R, Watanabe T, Inoue S, Kanauchi Y, et al. Complications of distal radius fractures treated by volar locking plate fixation. Orthopedics 2016; 39: e893–e896.

10. Stahl S, Schwartz O. Complications of K-wire fixation of fractures and dislocations in the hand and wrist. Arch Orthop Trauma Surg 2001; 121: 527–30.
11. Tubiana R. Early mobilization of fractures of the metacarpals and phalanges. Ann Chir Main 1983; 2: 293–97.
12. Lin CL, Lin YH, Chen AC. Buttressing angle of the double-plating fixation of a distal radius fracture: A finite element study. Med Biol Eng Comput 2006; 44: 665–73.
13. Cheng HY, Lin CL, Lin YH, Chao-Yu Chen A. Biomechanical evaluation of the modified double-plating fixation for the distal radius fracture. Clin Biomech 2007; 22: 510–17.
14. Trease C, McIff T, Toby EB. Locking versus nonlocking T-plates for dorsal and volar fixation of dorsally comminuted distal radius fractures: a biomechanical study. J Hand Surg Am 2005; 30: 756–63.
15. Brown CJ, Wang CJ, Yettramand AL, Procter P. Intramedullary nails with two lag screws. Clin Biomech 2004; 19: 519–25.
16. Aro HT, Chao EYS. Bone-healing patterns affected by loading, fracture fragment stability, fracture type, and fracture site compression. Clin Orthop Relat Res 1993; 293: 8–17.
17. Marshall, T, Momaya, A, Eberhardt, A, Chaudhari N, Hunt III, TR. Biomechanical comparison of volar fixed-angle locking plates for AO C3 distal radius fractures: titanium plates versus stainless steel with compression. J Hand Surg 2015; 40: 2032–2038.
18. Rogge RD, Adams BD, Goel VK. An analysis of bone stresses and fixation stability using a finite element model of simulated distal radius fractures. J Hand Surg 2002; 27: 86–92.
19. Lin Y, Sun MT, Chen AC, et al. Biomechanical analysis of volar and dorsal double locking plates for fixation in comminuted extra-articular distal radius fractures: A 3D finite element study. J Med Biol Eng 2012; 32: 349–56.
20. Osada D, Fujita S, Tamai K, Iwamoto A, Tomizawa K, Saotome K. Biomechanics in uniaxial compression of three distal radius volar plates. J Hand Surg Am 2004; 29: 446–51.
21. Shyamalan G, Theokli C, Pearse Y, Tennent D. Volar locking plates versus Kirschner wires for distal radial fractures - A cost analysis study. Injury 2009; 40: 1279–81.
22. Putnam MD, Meyer NJ, Nelson EW, Gesensway D, Lewis JL. Distal radial metaphyseal forces in an extrinsic grip model: Implications for postfracture rehabilitation. J Hand Surg 2000; 25: 469–75.
23. Jupiter JB. Complex articular fractures of the distal radius: Classification and management. J Am Acad Orthop Surg 1997; 5: 119–29.
24. Chao EY, Kasman RA, An KN. Rigidity and stress analysis of external fracture fixation devices - A theoretical approach. J Biomech 1982; 15: 971–83.